Spatially Resolved Signatures of Bidirectional Flows Observed in Inverted-Y Shaped Jets

C. J. Nelson[1,2] , N. Freij[3], S. Bennett[2], R. Erdélyi[2,4] , and M. Mathioudakis[1]

[1] Astrophysics Research Centre (ARC), School of Mathematics and Physics, Queen's University, Belfast BT7 1NN, UK; c.j.nelson@sheffield.ac.uk
[2] Solar Physics and Space Plasma Research Centre (SP2RC), School of Mathematics and Statistics, University of Sheffield, Hicks Building, Sheffield S3 7RH, UK
[3] Departament de Física, Universitat de les Illes Balears, E-07122 Palma de Mallorca, Spain
[4] Department of Astronomy, Eötvös Loránd University, Pázmány Péter sétány 1/A, H-1117 Budapest, Hungary

Abstract

Numerous apparent signatures of magnetic reconnection have been reported in the solar photosphere, including inverted-Y shaped jets. The reconnection at these sites is expected to cause localized bidirectional flows and extended shock waves; however, these signatures are rarely observed as extremely high spatial-resolution data are required. Here, we use Hα imaging data sampled by the Swedish Solar Telescope's CRisp Imaging SpectroPolarimeter to investigate whether bidirectional flows can be detected within inverted-Y shaped jets near the solar limb. These jets are apparent in the Hα line wings, while no signature of either jet is observed in the Hα line core, implying reconnection took place below the chromospheric canopy. Asymmetries in the Hα line profiles along the legs of the jets indicate the presence of bidirectional flows, consistent with cartoon models of reconnection in chromospheric anemone jets. These asymmetries are present for over two minutes, longer than the lifetimes of Rapid Blue Excursions, and beyond ± 1 Å into the wings of the line indicating that flows within the inverted-Y shaped jets are responsible for the imbalance in the profiles, rather than motions in the foreground. Additionally, surges form following the occurrence of the inverted-Y shaped jets. This surge formation is consistent with models, which suggests such events could be caused by the propagation of shock waves from reconnection sites in the photosphere to the upper atmosphere. Overall, our results provide evidence that magnetic reconnection in the photosphere can cause bidirectional flows within inverted-Y shaped jets and could be the driver of surges.

Key words: Sun: atmosphere – Sun: chromosphere – Sun: magnetic fields – Sun: photosphere

Supporting material: animations

1. Introduction

A huge range of potential signatures of magnetic reconnection in the solar photosphere have been reported in the literature. Transient, small-scale inverted-Y shaped jets, for example, have been widely studied over the past decade using high spatial and temporal resolution data. Such inverted-Y shaped jet events were first identified by Shibata et al. (2007) and manifest as bright regions on broadband Ca II H images (Morita et al. 2010; Nishizuka et al. 2011; Singh et al. 2012), as well as other chromospheric lines. Cartoon models presented in the literature (see, for example, Shibata et al. 2007; Singh et al. 2011) suggest that bidirectional reconnection outflows should exist in one footpoint of the inverted-Y shaped jets; however, hints that such bidirectional flows exist have only rarely been reported to date (see, for example, Zeng et al. 2016; Tian et al. 2018) as wide-band imaging data have typically been used to study these events. Recently, similar events have been identified at the footpoints of coronal loops (Chitta et al. 2017) and in sunspot light-bridges (Tian et al. 2018) indicating that inverted-Y shaped jets and, hence, magnetic reconnection may be prevalent throughout the solar photosphere. It is, therefore, important that further analysis of these events is conducted using high spatial and temporal resolution data in order to better understand their formation and evolution. We provide some steps in this direction in this article.

Further examples of reported reconnection events in the lower solar atmosphere are Ellerman bombs (EBs; Ellerman 1917) and quiet-Sun Ellerman-like brightenings (QSEBs; Rouppe van der Voort et al. 2016; Nelson et al. 2017). These events appear as small-scale (diameters often less than 1″), short-lived (lifetimes of less than 10 minutes) brightenings in the wings of the Hα line, often cospatial to regions of canceling magnetic flux (see, for example, Reid et al. 2016). Simulations of EBs have strongly supported the idea that such events form as a response to magnetic reconnection in the photosphere (see, for example, Nelson et al. 2013; Danilovic 2017; Hansteen et al. 2017).

Interestingly, both inverted-Y shaped jets and EBs have been reported to occur at the footpoints of larger-scale chromospheric events such as chromospheric anemone jets and surges (e.g., Roy 1973b; Watanabe et al. 2011; Yang et al. 2013a). Surges are columns of relatively cool material extending out from the solar chromosphere into the corona. These events typically have lengths of around 10″–70″ (Roy 1973a) and have been shown to consist of numerous distinct thin threads of material (Nelson & Doyle 2013; Li et al. 2016). Surges can be identified in chromospheric lines observed from the ground or in transition region and coronal lines sampled by satellites and often occur during interactions (e.g., through flux cancellation) between newly emerged magnetic flux and the background photospheric magnetic field (Chae et al. 1999; Guglielmino et al. 2010; Nóbrega-Siverio et al. 2016). As such, surges are considered to be formed as a response to magnetic reconnection in the lower solar atmosphere (for example, Roy 1973b; Guglielmino et al. 2010; Nóbrega-Siverio et al. 2016).

It should be noted, however, that only a small minority of the EBs reported in the literature appear to occur cospatial to these large chromospheric ejections. Indeed, Watanabe et al. (2011) found that only 2 of the 17 EBs they studied formed cospatial to surges. More recently, Reid et al. (2015) presented an observation showing short jets (not directly identified as surges by those authors) appearing to be driven by an EB observed in the Hα line wings. The reason why only a small percentage of reconnection events in the photosphere drive surges is currently unknown; however, it could speculatively be due to the local magnetic field topologies, the height of the reconnection, or the reconnection rate in the photosphere. This remains to be seen in future research using upcoming telescopes such as DKIST.

Although surges are suggested to be driven by magnetic reconnection in the lower solar atmosphere, they are not thought to be actual reconnection outflows. It has been hypothesized that slow magnetohydrodynamic (MHD) wave pulses are excited at the reconnection site and that these waves propagate up through the atmosphere to the transition region where they form shocks. These shocks create pressure gradients that drag the relatively dense material contained at the transition region to greater heights in the solar atmosphere, thereby creating the observed signatures of surges. This hypothesis was originally proposed by Shibata et al. (1982), who used pressure gradients in hydrodynamic simulations to drive waves into the upper solar atmosphere. Two-dimensional MHD simulations of magnetic reconnection in the lower solar atmosphere have confirmed the formation of such shocks following magnetic reconnection (see, for example, Kayshap et al. 2013; Takasao et al. 2013). Some observations have also found evidence for the occurrence of these processes in the solar atmosphere (De Pontieu et al. 2004; Tziotziou et al. 2005; Yang et al. 2014). Importantly, if this were the case, then a time lag (of the order minutes) should be present between the detection of reconnection processes in the photosphere and the occurrence of a surge, as the slow wave would have to propagate from the reconnection site into the transition region.

In this article, we analyze two inverted-Y shaped jets observed in AR 11506 at the solar limb using high-resolution Hα data in order to discern whether signatures of bidirectional flows are present. Sustained asymmetries in the Hα line profiles within the footpoints of the inverted-Y shaped jets imply the presence of bidirectional reconnection outflows, providing evidence that these events formed as a response to magnetic reconnection in the lower solar atmosphere. Additionally, both inverted-Y shaped jets appear to form at the footpoints of surges, which appear three minutes after the apparent onset of reconnection. We set out our work as follows: in Section 2 we introduce the data studied in this article; in Section 3 we present our results; in Section 4 we provide a discussion of our results before we draw our conclusions in Section 5.

2. Observations

In this article, we use ground-based data collected using the CRisp Imaging SpectroPolarimeter (CRISP; Scharmer 2006; Scharmer et al. 2008) at the Swedish 1 m Solar Telescope (Scharmer et al. 2003). These data sampled AR 11506 between 07:15:09 UT and 07:48:25 UT on 2012 June 21 (approximate coordinates of $x_c = 893''$ $y_c = -250''$) and have a pixel scale of $0''059$ (equating to around 43 km in the horizontal plane) and a cadence of 7.7 s, following reduction using the Multi-Object Multi-Frame Blind Deconvolution (MOMFBD; van Noort et al.

2005) method. The reduction employed the standard CRISP reduction pipeline (discussed by de la Cruz Rodríguez et al. 2015), including the post-MOMFBD correction for differential stretching (Henriques 2012). A total of 35 wavelength positions across the Hα line profile (where 6562.8 Å is now used throughout the remainder of this article as a reference [0 Å] wavelength) were observed in the range $[-2 \text{ Å}, +1.2 \text{ Å}]$.

In order to supplement the CRISP data, we also used space-borne data sampled by the *Solar Dynamics Observatory*'s Atmospheric Imaging Assembly (*SDO*/AIA; Lemen et al. 2012). These data are analyzed between 07:15:09 UT and 08:19:48 UT in order to include the full evolution of the second event discussed in this article. We use 1600 and 1700 Å data, with a cadence of 24 s, to investigate whether brightenings were observed in the lower atmosphere and three EUV channels (304 Å, 171 Å, and 211 Å), with a cadence of 12 s, to deduce the response of the upper atmosphere. All of these data have a pixel scale of approximately $0''6$ (corresponding to around 430 km in the horizontal scale). The data analysis presented here was conducted, in part, using the CRISPEX tool (Vissers & Rouppe van der Voort 2012). It should be noted that although a careful alignment between the *SDO*/AIA data and the CRISP data was completed to confirm that the ejections observed in the EUV channels corresponded to those detected in the ground-based data, the analysis presented here was conducted on the nonrotated data in order to limit errors induced by interpolating the images. In Figure 1, we plot a time-series of context images displaying the FOV analyzed here as observed by the *SDO*/AIA 304 Å (top row), 171 Å (middle row), and 211 Å (bottom row) filters. The labeled white arrows in the top row indicate the locations of the two surges studied in Section 3.2.

3. Results

3.1. Properties of the Inverted-Y Shaped Jets

We begin our analysis by investigating two inverted-Y shaped jets identified in the wings of the Hα line (from around ±0.8 Å outwards). The evolution of the lower solar atmosphere during and following the first inverted-Y shaped jet studied here (where the inverted-Y shaped jet and apparently associated surge are known subsequently as "Event A" and "Surge A," respectively) was evident between 07:25 UT and 07:33 UT and is plotted in Figure 2 for three positions in the Hα line profile. Event A is clearly observable in the line wings (indicated by the arrows in the top and bottom rows) in the first three columns, however, no evidence of this structure is apparent in the Hα line core. This inverted-Y shaped jet had an apparent vertical extent of approximately 1″ and a footpoint separation of around 1″. These values align well with the statistical properties of chromospheric anemone jets (as reported by Nishizuka et al. 2011). Chromospheric anemone jets have been widely associated with magnetic reconnection, both observationally (as discussed by, e.g., Shibata et al. 2007; Morita et al. 2010; Singh et al. 2011) and numerically (Yang et al. 2013b). A similar plot is included for the second inverted-Y shaped jet studied here ("Event B" and "Surge B") in Figure 3. Event B was visible between approximately 07:28 UT and 07:34 UT and had similar spatial properties to Event A. The evolution of these events is plotted in the online movies associated with this article.
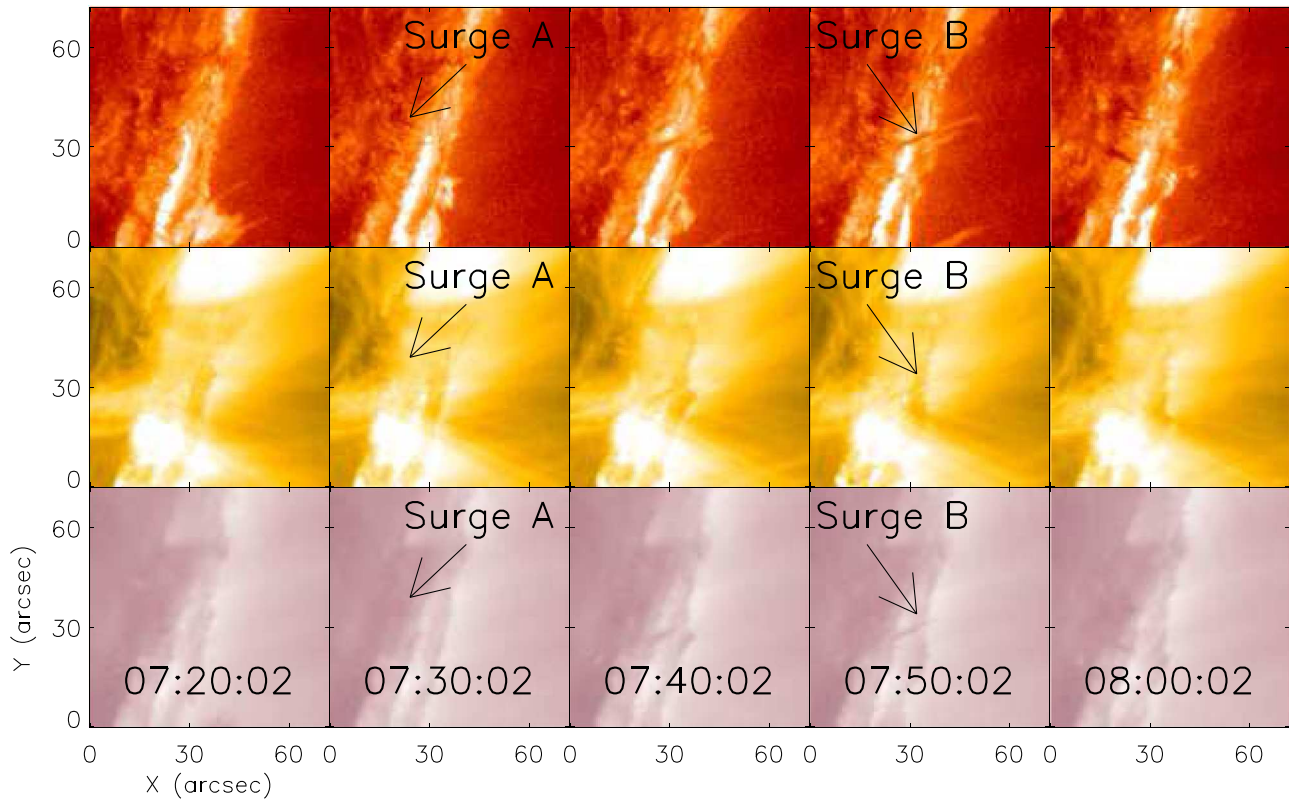
Figure 1. Time-series of *SDO*/AIA context images displaying the evolution of the FOV studied here with the intensity log-scaled to enhance the contrast. The top, middle, and bottom rows plot data sampled by the 304 Å, 171 Å, and 211 Å filters, respectively. The locations of the surges analyzed later in this article ("Surge A" itself is not easily observed in these zoomed-out context images due to its relatively small size), which appear as absorption features in each of the *SDO*/AIA channels, are indicated by the appropriately labeled white arrows in the top (304 Å) row.

In order to further investigate these inverted-Y shaped jets, we analyzed the Hα line profiles within their footpoints. Cartoon models of such jets imply that signatures of bidirectional flows (e.g., asymmetric line profiles) would be expected along the length of the jets (examples are presented in, e.g., Shibata et al. 2007; Singh et al. 2011). These models suggest that such bidirectional flows are caused by magnetic reconnection, which occurs within one leg of the jet. Although the associated asymmetries would perhaps be more prominent closer to disk center due to the expected vertical nature of the magnetic reconnection, one would still expect some signature at the limb as it is unlikely that any reconnection outflows would be purely in the plane-of-sky. In the left-hand panels of Figure 4, we plot Event A at three positions within the Hα line profile and the normalized line profiles at four points along the leg of the inverted-Y shaped jet. The four spatial positions at which the line profiles were calculated are indicated by colored crosses on each image. The right-hand panels plot the same information for Event B.

At the base of Event A, strong asymmetries are detected in the line profiles, with larger intensity enhancements being measured in the red wing of the line when compared to the blue wing. These redshifts (red and orange profiles in Figure 4) are consistent with material flowing away from the observer. Symmetric profiles are then observed at the center of the leg (light blue line in Figure 4) before strong asymmetries manifesting as enhancements in the blue wing intensities (e.g., blueshifted profiles) are measured at the top of the leg (purple line in Figure 4), indicative of material moving toward the observer. Similar results are found for Event B, however,

these, are perhaps more striking with the purple and red profiles displaying 40% increases in intensity in one wing only. It should be noted that the asymmetries extend out to -2 Å (as can be seen in Figure 4), beyond the typical spectral extent of RBEs (Sekse et al. 2012). These results suggest that spatially resolved bidirectional flows may be present within the footpoint of the jet, analogous to the cartoon models of chromospheric anemone jets (see Shibata et al. 2007; Singh et al. 2011). We stress that the identification of bidirectional flows within the legs of the inverted-Y shaped jets at the footpoints of the surges do not correspond to the up- and downflows identified within surges themselves (e.g., Brooks et al. 2007; Madjarska et al. 2009).

In order to better understand whether these asymmetries originate from bidirectional flows within the inverted-Y shaped jets themselves or are caused by line-of-sight effects, we conduct an analysis of the temporal evolution of the Hα line profiles. Specifically, it is important to examine whether these asymmetries could be caused by the supposition of EB-like symmetric wing emission profiles with asymmetric wing absorption profiles caused by motion of material in the foreground (e.g., Rapid Blue Excursions; RBEs). In Figure 5, we plot the difference in intensity between the red and blue wings (± 0.946 Å) through time for the purple and red pixels plotted in Figure 4. For both Event A and Event B, the asymmetries are sustained throughout the lifetimes of the events, which are longer than the average lifetimes of RBEs (see, for example, Sekse et al. 2012 where typical RBEs were found to be detectable for less than 90 s). As the lifetimes of these inverted-Y shaped jets are larger than those associated
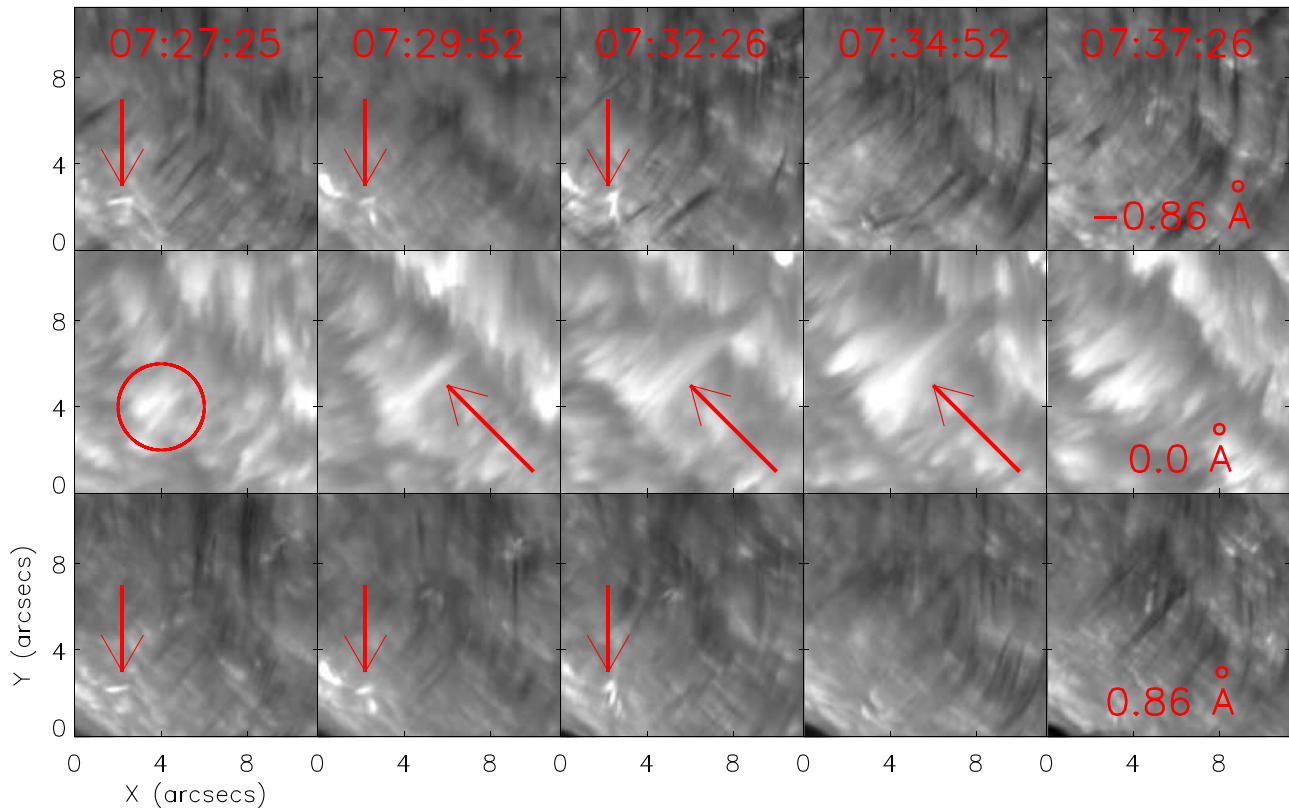
Figure 2. Evolution of Event A through its lifetime sampled at three positions within the Hα line profile. The top row plots the Hα blue wing (−0.86 Å), the middle row plots the Hα line core, and the bottom row plots the Hα red wing (+0.86 Å). The arrows overlaid on the blue and red wing images indicate the inverted-Y shaped jet detected in the lower atmosphere which is studied in detail in Section 3.1. The associated surge is indicated by the arrows in the Hα line core panels. The red circle in the left-hand Hα line core panel identifies a small bright patch detected prior to Surge A (discussed in Section 3.2). The animation is made from images corresponding to slightly different Hα wing positions (±0.946 Å) and having a longer baseline (from 7:21 to 7:47 UT) than the static figure. Arrows in the three panels of the animation correspond to the inverted-Y shaped jet and the associated surge as in the static version.

(An animation of this figure is available.)

with RBEs, we can refute the hypothesis that these asymmetries could be caused by the supposition of symmetric emission and asymmetric absorption profiles.

The strong asymmetries within the individual line profiles plotted in Figure 4 (particularly evident in the red and purple lines in the right-hand panel where one wing is in emission and one wing is at the background intensity level) distinguish these inverted-Y shaped jets from both EBs (see Nelson et al. 2015 for an analysis of EBs in the same data set) and QSEBs (as discussed by Rouppe van der Voort et al. 2016; Nelson et al. 2017). The relatively small intensity enhancements (only 140% of the background intensity) of the inverted-Y shaped jets are also lower than the thresholds used to identify EBs in the modern literature (see, for example, Nelson et al. 2015; Vissers et al. 2015). To further investigate the chromospheric anemone jets, we searched for signatures of these events in the SDO/AIA 1600 Å and 1700 Å channels. No increased emission was detected in either filter during the occurrence of the inverted-Y shaped jets which, again, distinguishing these events from EBs.

As the inverted-Y shaped jets brighten in the wings of the Hα line profile, and not in the line core, it is likely that the magnetic reconnection which drives these events takes place low down in the solar atmosphere, potentially in the photosphere (for a discussion of small-scale reconnection events in the lower solar atmosphere see Young et al. 2018). The models of Takasao et al. (2013) suggest that reconnection at such

heights (i.e., below the $\beta = 1$ layer) would generate slow magnetoacoustic wave pulses which would shock in the upper chromosphere to lift the transition region to greater heights, which we could observe as a surge. We examine potential links between these inverted-Y shaped jets and surges in the following subsection.

3.2. Potential Links to Surges

Both inverted-Y shaped jets studied in this article appeared to have some links to surges observed in the Hα line core. For Event A, a surge was observed to form at the same apparent spatial location a few minutes after the onset of the inverted-Y shaped jet. Initially, a small brightening (indicated by the red circle on the first panel of the middle row in Figure 2) was observed in the Hα line core at around 07:27:25 UT before a surge extended out into the upper atmosphere from this location. By 07:38:13 UT the surge had receded back to the chromospheric canopy. The evolution of Surge A through time in the Hα line core can be seen in the middle row of Figure 2. Surge A evolved in two apparently distinct phases, specifically the initial rise phase and the subsequent descending phase. At the beginning of the rise phase, a small bright patch was present in the Hα line core (enclosed in the red circle in the first panel of the middle row in Figure 2) at the footpoint of the event. This bright patch had a length of around 2″, a width of approximately 1″, a lifetime of around 1 minute, and faded as
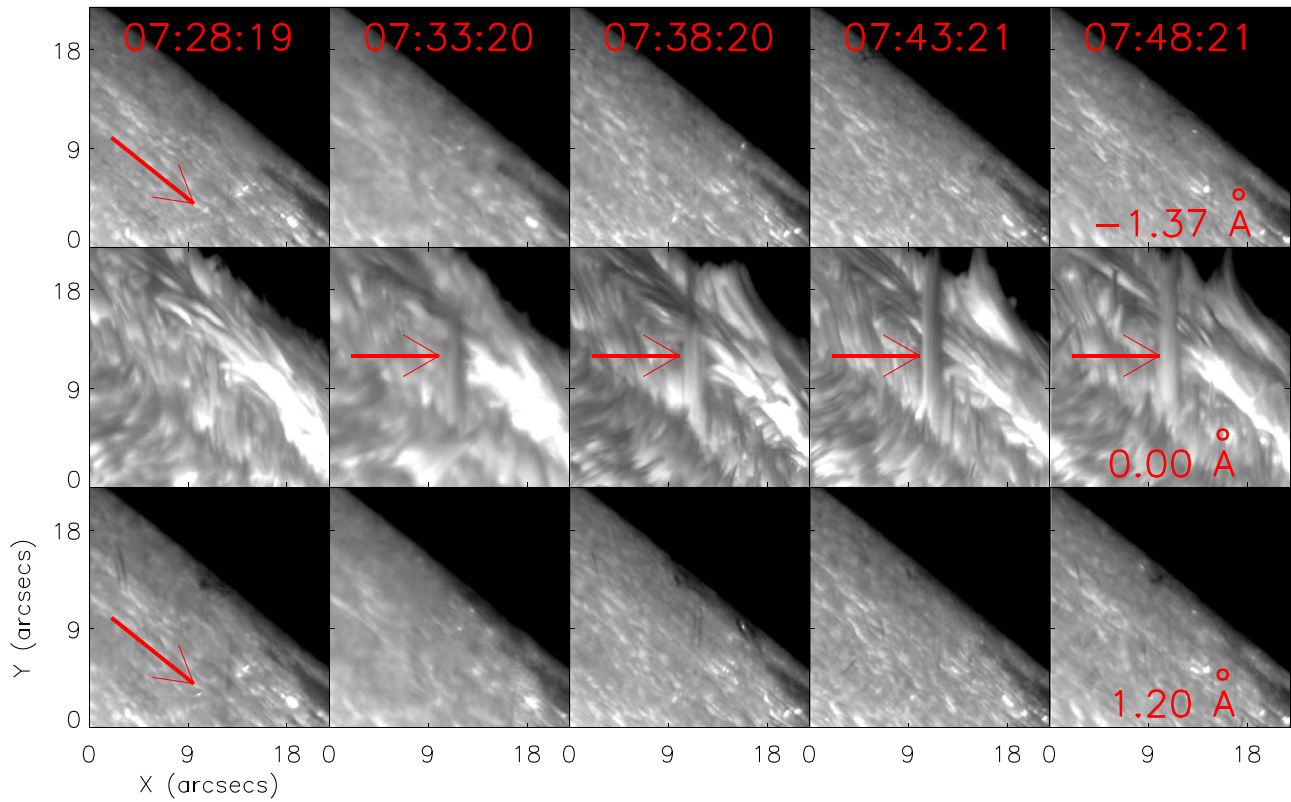
Figure 3. Similar to Figure 2 but for Event B. The Hα line wing positions are now −1.37 Å and +1.20 Å to better highlight the inverted-Y shaped jet. The inverted-Y shaped jet (indicated by red arrows in the line wing images and studied in detail in Section 3.1) is faint in comparison to nearby EBs. The surge associated with this jet extends outside of the CRISP FOV (right-hand panel in the middle row). The animation is made from images corresponding to slightly different Hα wing positions (±1.29 Å) and having a longer baseline (from 7:21 to 7:47 UT) than the static figure. Arrows in the three panels of the animation correspond to the inverted-Y shaped jet and the associated surge as in the static version.
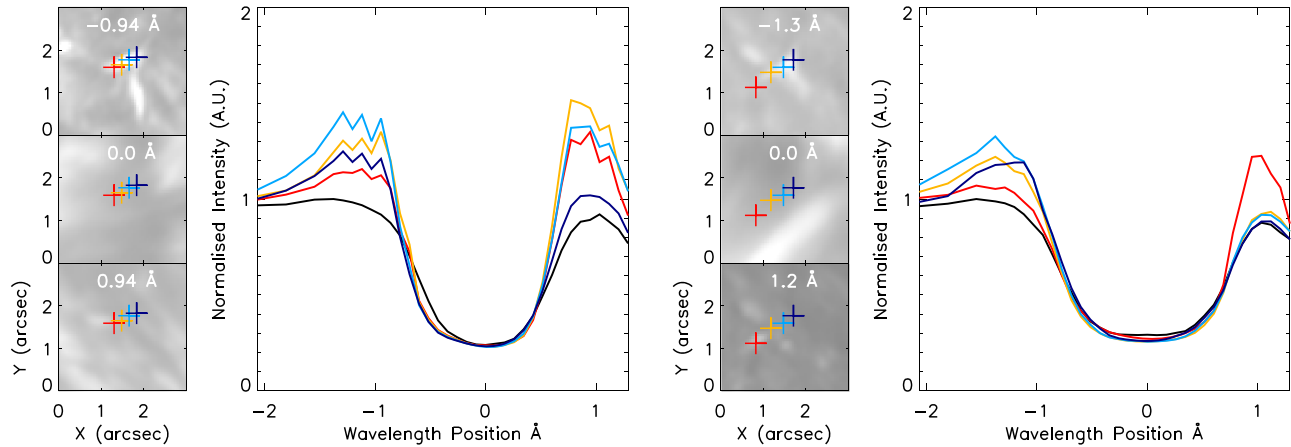
(An animation of this figure is available.)

Figure 4. (Left-hand panels) Event A plotted in three wavelengths (specific wavelength positions indicated in the individual panels) in the Hα line profile at 07:30:53 UT. The crosses indicate pixels analyzed along one leg of the inverted-Y shaped jet. The spectral profiles for the background (black line) and the four positions along the length of one leg of the inverted-Y shaped jet analyzed here are plotted normalized against the background intensity. A clear transition from red- to blueshifted profiles occurs from the bottom to the top of the leg. (Right-hand panels) Same but for Event B. Again, a clear asymmetry in the profiles (from blue to red) can be observed along the leg of the jet.

Surge A began to increase in length. Throughout the rise phase, Surge A manifested as a thin, collimated structure (indicated by the red arrows in the second and third panels of the middle row of Figure 2), with a width of around $2\rlap{.}''2$. The peak length of the structure was around $8\rlap{.}''1$, which was reached at 07:32:41 UT. This makes Surge A a shorter than average surge (Roy 1973a).

After Surge A had reached its peak length and began to recede, it began to expand radially. This behavior is similar to the expected evolution of surges (or jets) when magnetic reconnection takes place in the photosphere or lower chromosphere, according to the simulations of Takasao et al. (2013). In this scenario, slow wave pulses, formed due to the occurrence of magnetic reconnection in the lower solar atmosphere, shock
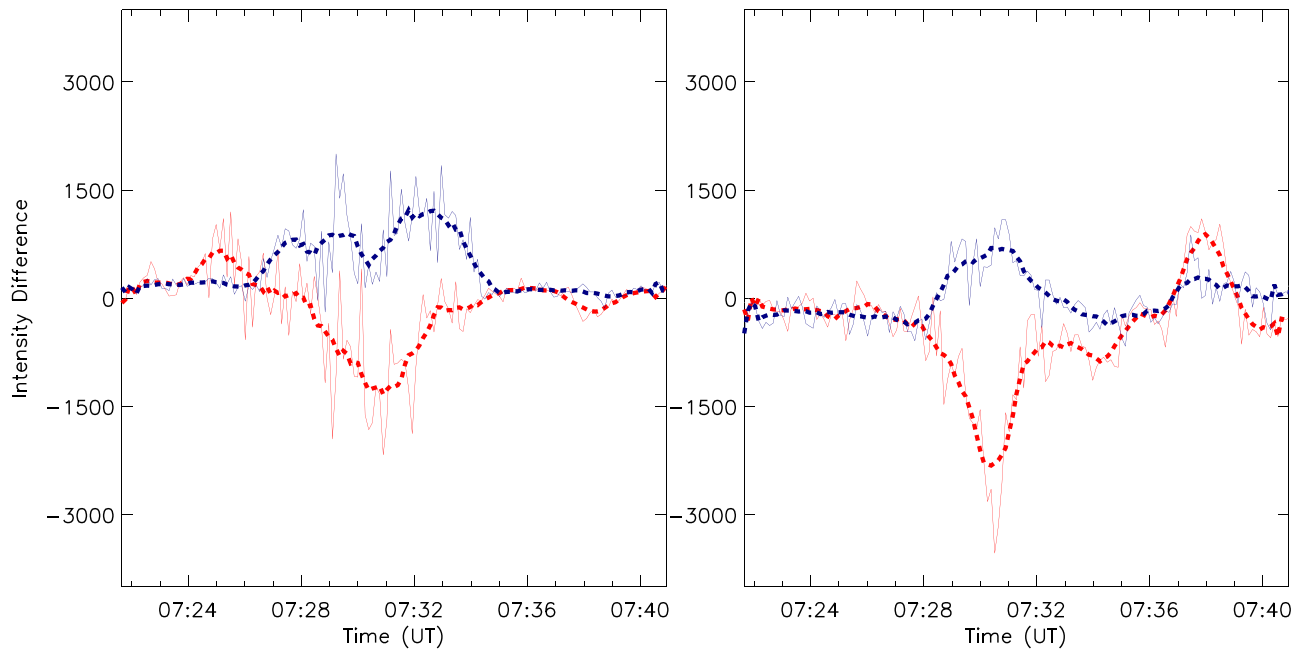
Figure 5. Intensity difference between the blue wing and the red wing (Int[−0.946 Å]–Int[0.946 Å]) through time for two pixels at the top (purple line) and bottom (red line) of the inverted-Y shaped jets. Event A is plotted in the left-hand panel and Event B is plotted in the right-hand panel. The colors correspond to pixels denoted by the same colored crosses plotted in Figure 4. The overlaid dashed lines are running difference plots with smoothing applied over 10 frames (i.e., 77 s). These plots clearly display that the asymmetries within the inverted-Y shaped jets are sustained for around 8 minutes for Event A and 6 minutes for Event B.

in the transition region leading to the ejection of chromospheric material, initially along the magnetic field lines, which we observe as a surge. The peak width of Surge A was approximately 5″ (see the fourth panel of the middle row in Figure 2) before it disappeared from view entirely (fifth panel of the Hα line core row of Figure 2) as the surge material fell back under gravity to normal heights.

Surge B, the surge apparently associated with Event B, was first observable in the Hα line core at 07:30:38 UT and lived beyond the end of the CRISP observations. As, here, the surge is resolvable in a range of SDO/AIA filters, the lack of high-resolution ground-based data sampling the descending phase of the surge does not limit our ability to infer information about its evolution. Through analysis of the SDO/AIA 304 Å channel, we were able to identify that Surge B receded back to presurge heights at around 07:54:20 UT, giving it a total lifetime of around 24 minutes. As can be seen in the center row of Figure 3, the surge extended out of the CRISP field of view (FOV) meaning the spatial properties of the structure were also measured using the SDO/AIA 304 Å channel. The peak length of Surge B was 23″ and its width varied between 2″.5 and 3″.5 through time. No expansion of the surge material was detected during the descending phase.

In terms of temporal evolution, Surge B was slightly more complex than Surge A. In Figure 6, we plot a time-distance diagram constructed by sampling the Hα line core intensity along the length of the surge. The exact positioning of the slit used to construct the diagram is indicated by the black line in the right-hand panels of Figure 7. The event classified as Surge B here appears to be made-up of two successive surges which occurred at the same location (labeled as "B1" and "B2") around six minutes apart. The first ejection contained within the surge was relatively short, with a length of around 8″; however, the second ejection reached much higher into the atmosphere, to heights of around 23″ (measured using the 304 Å channel

from SDO/AIA). Both surges extend with an apparent upward (plane-of-sky) velocity of around 30 km s^{-1} (33 km s^{-1} and 28 km s^{-1} for surges B1 and B2, respectively), slower than the surges discussed by Kayshap et al. (2013). Surge B1 also receded at a similar apparent velocity (see Figure 6). The occurrence of multiple ejections along the same trajectory implies the occurrence of a repetitive driver, in this case thought to be magnetic reconnection in the lower solar atmosphere. Such repetition has been observed in EBs (Vissers et al. 2015), UV bursts (Nelson et al. 2016), and explosive events (Chae et al. 1998).

When observed with the SDO/AIA EUV filters, the main bodies of both surges appeared in absorption throughout their lifetimes, and no increased emission was detected at their footpoints or tips during their rise or descent phases (see Figure 1). The fact that both surges appeared in absorption implies the presence of higher levels of neutral hydrogen along the line of sight (Williams et al. 2013). Additionally, no bright material was present at the tips of these events, unlike the wave-driven events recently studied by Reid et al. (2018), suggesting no significant heating occurring. These observations match well with the hypothesis that relatively cool, chromospheric material is lifted into the upper atmosphere by slow shock pulses at the transition region (although the SDO/AIA data themselves do not rule out other scenarios). Interestingly, Surge B appears to be well aligned to a coronal loop arcade, which can be identified in 171 Å images (see panels three and four of the middle row of Figure 1). The material contained within Surge B is seemingly confined within the lower portions of the loop during both its rise and descent phases; however, direct alignment is difficult due to the relatively low spatial resolution of the SDO/AIA data.

In order to further analyze both surges, we investigated whether any rotational motions were evident during their evolutions or whether the inclination angle of the surges could
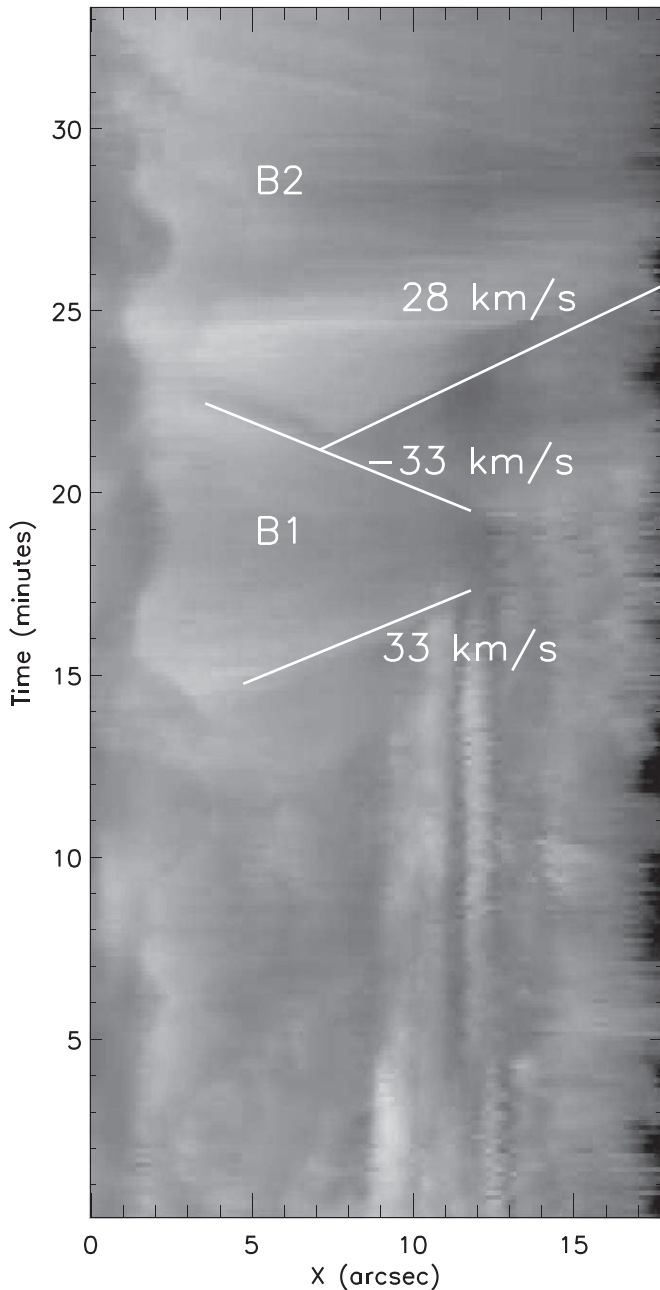
Figure 6. Distance–time plot displaying the evolution of the length of Surge B plotted with a natural log intensity scale. The black line in the right-hand panels of Figure 7 indicate the pixels used to construct this plot. Time zero corresponds to 07:15:09 UT (i.e., the beginning of the observational time-series). The white lines indicate the position of the tops of the surge material through time for ease of the reader (and thus represent the apparent velocity). The recurrent nature of Surge B is evident, with the two repetitions being indicated by the labels "B1" and "B2." The apparent upward (positive) and downward (negative) velocities of the surges are indicated by the labeled white lines overlaid on the plot.

be inferred. Previous research has indicated that the rotation of solar jets can be related to the degree of twist within the reconnection site at their footpoints (see, for example, Liu et al. 2018). Therefore, a lack of observable twist within the surges could add support to the hypothesis that these events formed as a response to upwardly propagating slow shock pulses, rather than the release of free magnetic energy stored within twisted magnetic field lines. Doppler maps were constructed through

single Gaussian fitting to the observed Hα line profiles, in the wavelength range [-1.032 Å, $+1.032$ Å], at each pixel in the FOV. Velocities were estimated by comparing the position of the center of the fitted Gaussian to 6562.8 Å, the assumed rest wavelength of Hα. This analysis identified no significant (greater than ± 1 km s^{-1}) line-of-sight velocities cospatial to either event in terms of either rotation or inclination.

In Figure 7, we plot the locations of the two surges analyzed here in the chromospheric Hα line core (larger panels) in comparison to the inverted-Y shaped jets in the Hα line wings (smaller panels). All frames are plotted at approximately 07:30:38 UT. The black lines in the Hα line core images indicate the axis of the surges and the white boxes outline the FOV plotted in the line wings at their footpoints in the smaller panels. The specific line wing positions are denoted on each individual panel. The inverted-Y shaped jets are both apparent at the footpoints of the surges. It should be noted that for Surge B, the inverted-Y shaped jet is only evident prior to B1. Only a small brightening in the blue wing of the Hα line with an indistinct shape is detectable prior to B2; however, this could be due to a reduction in the seeing level during this time.

As can be seen in Figures 2 and 3, the inverted-Y shaped jets occurred prior to and during the initial extension phases of both surges. Both inverted-Y shaped jets are first observable around three minutes prior to the formation of the surges. By measuring the height difference between the reconnection site (where the slow-mode wave pulse is conjectured to be excited) and the transition region (where the slow-mode shock pulse theoretically lifts the surge material), we would be able to calculate the propagation speed of the slow wave pulse; however, as this height difference is not known and cannot be measured, here we instead use potential height differences to estimate representative speeds of the propagating wave pulse. If we assume representative height differences of 1000, 1500, and 2000 km, we are able to estimate potential slow wave propagation speeds of 5.5, 8.3, and 11.1 km s^{-1}. These values are in line with the expected propagation speed of slow MHD waves in the lower solar atmosphere. It is possible, therefore, that these surges are formed as a response to magnetic reconnection in the lower solar atmosphere.

4. Discussion

In this article, we have presented an analysis of two inverted-Y shaped jets detected in the wings of Hα line scans sampled by the CRISP instrument (see Figures 2 and 3). These inverted-Y shaped jets had similar properties (lifetimes, lengths, and footpoint separations) to chromospheric anemone jets (see, for example, Shibata et al. 2007; Nishizuka et al. 2011) as well as other inverted-Y shaped jets (e.g., Tian et al. 2018). The intensity enhancements measured at the locations of these jets are relatively faint, with a maximum intensity enhancement of around 140% (Figure 4). This is well below the 150% threshold value often used for EBs (e.g., Nelson et al. 2015).

Strong asymmetries in the Hα line profiles were measured in the legs of both inverted-Y jets (often with intensities 20%–30% higher in one wing over another). These asymmetries progressed from blue to red along the length of the inverted-Y shaped jets implying that bidirectional flows were occurring. Such flows would be expected if these inverted-Y shaped jets were formed due to magnetic reconnection (discussed by, for example, Shibata et al. 2007). These asymmetries last for the entire lifetime of the inverted-Y shaped jets (9 minutes and 6
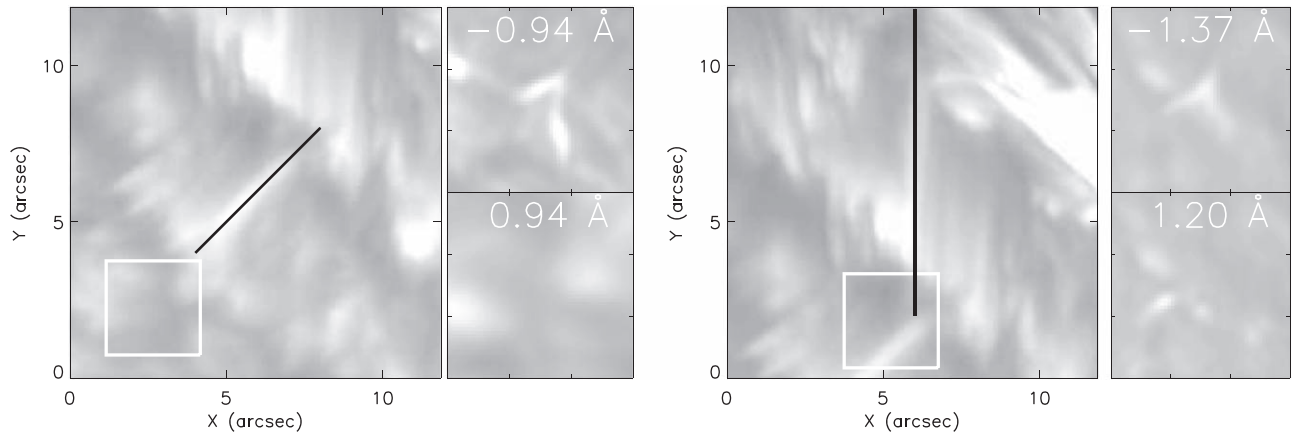
Figure 7. (Left-hand panels) The chromospheric Hα line core (large panel) and photospheric Hα line wing (smaller panels) signatures of Surge A and its footpoints at 07:30:38 UT. The black line in the left-hand panel indicates the positioning and orientation of the surge. The white boxes indicate the FOV plotted in the smaller panels. (Right-hand panels) Same but for Surge B. The black line overlaid on the Hα line core image indicates the axis of the slit used to construct the distance–time diagram plotted in Figure 6. The inverted-Y shaped jets are clearly evident at the footpoint of both surges in the blue wing of the Hα line in this time step.

minutes for Event A and Event B, respectively) indicating that they are physical in nature rather than due to a supposition of symmetric EB-like profiles and asymmetric RBE-like profiles (which would have much shorter lifetimes). In a manner similar to EBs, no brightening signature is observed in the Hα line core during these jets implying that magnetic reconnection took place low down in the atmosphere, potentially in the photosphere.

Both inverted-Y shaped jets appeared to form at the footpoints of chromospheric surges. The surge associated with Event A was a relatively short event, with a length of 8″, and had a lifetime of just under 11 minutes. After this event had reached its peak height and begun to contract, it started to expand radially in a manner similar to the surges presented in the simulations of Takasao et al. (2013). The surge associated with Event B was longer, with a maximum length of 23″; however, it appeared to be comprised of two consecutive surges at the same location. Both surges appeared in absorption in *SDO*/AIA EUV data implying the presence of H bound-free absorption (i.e., an increase in the neutral hydrogen density, consistent with the hypothesis of chromospheric material being lifted higher into the atmosphere) as was discussed by Williams et al. (2013). A localized bright region observed at the footpoint of Surge A in the Hα line core could be indicative of some heating at the chromospheric or transition region layers; however, no brightening was evident in *SDO*/AIA data. Interestingly, a three minute delay was also observed between the detection of the inverted-Y shaped jets and the formation of the surges potentially corresponding to the time required for the slow-mode waves to propagate from the reconnection site to the chromosphere.

5. Conclusions

Overall, our results imply that these two inverted-Y shaped jets are formed as a response to magnetic reconnection in the lower solar atmosphere. One of the main advances of this work over previous works is the detection of bidirectional flows, which we were able to measure along the legs of the inverted-Y shaped jets using transition of blue to red asymmetries. Such flows would only be detectable in extremely high-resolution data such as those sampled by the CRISP instrument. Surges appear to form at the same locations as the inverted-Y shaped

jets potentially further hinting to the formation of magnetic reconnection in the solar photosphere. However, we should note that our small sample size does not conclusively link inverted-Y shaped jets to surges meaning future work must be conducted. A larger statistical sample should be conducted in the future to provide further evidence about links between these two phenomena.

Future work should aim to study a larger statistical sample of inverted-Y shaped jets to identify how frequently such features form cospatial to surges. Additionally, it would be interesting to study how the inclination angles of any associated surges relates to the flow patterns detected within the inverted-Y shaped jets. Such work would require extremely high-resolution spectroscopic data acquired during a period of good seeing due to the small-spatial scales and low intensity enhancements of these events. DKIST should offer excellent data in this regard.

ORCID iDs

C. J. Nelson ⓘ https://orcid.org/0000-0003-1400-8356
R. Erdélyi ⓘ https://orcid.org/0000-0003-3439-4127
M. Mathioudakis ⓘ https://orcid.org/0000-0002-7725-6296

References

Brooks, D. H., Kurokawa, H., & Berger, T. E. 2007, ApJ, 656, 1197
Chae, J., Qiu, J., Wang, H., & Goode, P. R. 1999, ApJL, 513, L75
Chae, J., Wang, H., Lee, C.-Y., Goode, P. R., & Schühle, U. 1998, ApJL, 497, L109
Chitta, L. P., Peter, H., Solanki, S. K., et al. 2017, ApJS, 229, 4
Danilovic, S. 2017, A&A, 601, A122

de la Cruz Rodríguez, J., Löfdahl, M. G., Sütterlin, P., Hillberg, T., & Rouppe van der Voort, L. 2015, A&A, 573, A40
De Pontieu, B., Erdélyi, R., & James, S. P. 2004, Natur, 430, 536
Ellerman, F. 1917, ApJ, 46, 298
Guglielmino, S. L., Bellot Rubio, L. R., Zuccarello, F., et al. 2010, ApJ, 724, 1083
Hansteen, V. H., Archontis, V., Pereira, T. M. D., et al. 2017, ApJ, 839, 22
Henriques, V. M. J. 2012, A&A, 548, A114
Kayshap, P., Srivastava, A. K., & Murawski, K. 2013, ApJ, 763, 24
Lemen, J. R., Title, A. M., Akin, D. J., et al. 2012, SoPh, 275, 17
Li, Z., Fang, C., Guo, Y., et al. 2016, ApJ, 826, 217
Liu, J., Erdélyi, R., Wang, Y., & Liu, R. 2018, ApJ, 852, 10
Madjarska, M. S., Doyle, J. G., & de Pontieu, B. 2009, ApJ, 701, 253
Morita, S., Shibata, K., UeNo, S., et al. 2010, PASJ, 62, 901
Nelson, C. J., & Doyle, J. G. 2013, A&A, 560, A31
Nelson, C. J., Doyle, J. G., & Erdélyi, R. 2016, MNRAS, 463, 2190
Nelson, C. J., Freij, N., Reid, A., et al. 2017, ApJ, 845, 16
Nelson, C. J., Scullion, E. M., Doyle, J. G., Freij, N., & Erdélyi, R. 2015, ApJ, 798, 19
Nelson, C. J., Shelyag, S., Mathioudakis, M., et al. 2013, ApJ, 779, 125
Nishizuka, N., Nakamura, T., Kawate, T., Singh, K. A. P., & Shibata, K. 2011, ApJ, 731, 43
Nóbrega-Siverio, D., Moreno-Insertis, F., & Martínez-Sykora, J. 2016, ApJ, 822, 18
Reid, A., Henriques, V. M. J., Mathioudakis, M., & Samanta, T. 2018, ApJL, 855, L19
Reid, A., Mathioudakis, M., Doyle, J. G., et al. 2016, ApJ, 823, 110
Reid, A., Mathioudakis, M., Scullion, E., et al. 2015, ApJ, 805, 64
Rouppe van der Voort, L. H. M., Rutten, R. J., & Vissers, G. J. M. 2016, A&A, 592, A100

Roy, J.-R. 1973a, SoPh, 32, 139
Roy, J. R. 1973b, SoPh, 28, 95
Scharmer, G. B. 2006, A&A, 447, 1111
Scharmer, G. B., Bjelksjo, K., Korhonen, T. K., Lindberg, B., & Petterson, B. 2003, Proc. SPIE, 4853, 341
Scharmer, G. B., Narayan, G., Hillberg, T., et al. 2008, ApJL, 689, L69
Sekse, D. H., Rouppe van der Voort, L., & De Pontieu, B. 2012, ApJ, 752, 108
Shibata, K., Nakamura, T., Matsumoto, T., et al. 2007, Sci, 318, 1591
Shibata, K., Nishikawa, T., Kitai, R., & Suematsu, Y. 1982, SoPh, 77, 121
Singh, K. A. P., Isobe, H., Nishizuka, N., Nishida, K., & Shibata, K. 2012, ApJ, 759, 33
Singh, K. A. P., Shibata, K., Nishizuka, N., & Isobe, H. 2011, PhPl, 18, 111210
Takasao, S., Isobe, H., & Shibata, K. 2013, PASJ, 65, 62
Tian, H., Yurchyshyn, V., Peter, H., et al. 2018, ApJ, 854, 92
Tziotziou, K., Tsiropoula, G., & Sütterlin, P. 2005, A&A, 444, 265
van Noort, M., Rouppe van der Voort, L., & Löfdahl, M. G. 2005, SoPh, 228, 191
Vissers, G., & Rouppe van der Voort, L. 2012, ApJ, 750, 22
Vissers, G. J. M., Rouppe van der Voort, L. H. M., Rutten, R. J., Carlsson, M., & De Pontieu, B. 2015, ApJ, 812, 11
Watanabe, H., Vissers, G., Kitai, R., Rouppe van der Voort, L., & Rutten, R. J. 2011, ApJ, 736, 71
Williams, D. R., Baker, D., & van Driel-Gesztelyi, L. 2013, ApJ, 764, 165
Yang, H., Chae, J., Lim, E.-K., et al. 2013a, SoPh, 288, 39
Yang, H., Chae, J., Lim, E.-K., et al. 2014, ApJL, 790, L4
Yang, L., He, J., Peter, H., et al. 2013b, ApJ, 777, 16
Young, P. R., Tian, H., Peter, H., et al. 2018, SSRv, 214, 120
Zeng, Z., Chen, B., Ji, H., Goode, P. R., & Cao, W. 2016, ApJL, 819, L3